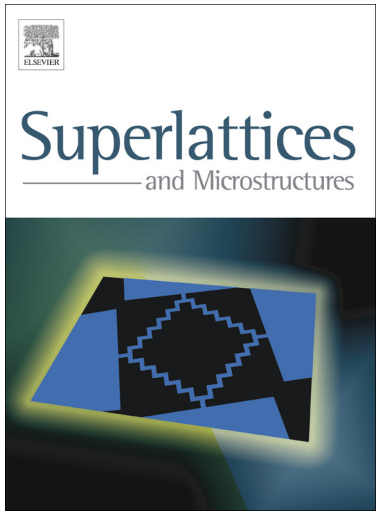

Structural and Optical Properties of Au-Catalyzed SiNWs Grown Using Pulsed Plasma-Enhanced Chemical Vapour Deposition

H.F. Al-Taay, M.A. Mahdi, D. Parlevliet, Z. Hassan, P. Jennings

PII: S0749-6036(13)00185-7
DOI: http://dx.doi.org/10.1016/j.spmi.2013.06.008
Reference: YSPMI 2924

To appear in: *Superlattices and Microstructures*

Received Date: 6 February 2013
Accepted Date: 10 June 2013

Please cite this article as: H.F. Al-Taay, M.A. Mahdi, D. Parlevliet, Z. Hassan, P. Jennings, Structural and Optical Properties of Au-Catalyzed SiNWs Grown Using Pulsed Plasma-Enhanced Chemical Vapour Deposition, *Superlattices and Microstructures* (2013), doi: http://dx.doi.org/10.1016/j.spmi.2013.06.008

Structural and Optical Properties of Au-Catalyzed SiNWs Grown Using Pulsed Plasma-Enhanced Chemical Vapour Deposition

H.F. Al-Taay[1,*], M.A. Mahdi[2], D. Parlevliet[1], Z. Hassan[2], P. Jennings[1]

1. School of Engineering and Energy, Murdoch University, South St., Murdoch,WA6150, Australia.

2. Nano-Optoelectronics Research Technology Laboratory (N.O.R), School of Physics, Universiti Sians Malaysia, Penang, Malaysia.

*Corresponding author (H.F. Al-Taay): H/P: 0061-422411653, E-mail: hanaa_flayeh@yahoo.com

Abstract

Silicon nanowires (SiNWs) were grown on indium tin oxide-coated glass substrates using pulsed plasma-enhanced chemical vapour deposition (PPECVD) with gold (Au) as a catalyst. Various thicknesses of Au thin films ranging from 10 nm to 100 nm were deposited on the substrates by thermal evaporation. The surface morphological study of the prepared wires showed that the wire diameter increased as the catalyst film thickness increased. The X-ray diffraction patterns of the prepared SiNWs illustrated that the grown wires had cubic phase, and the crystallinity was enhanced as the catalyst thickness increased. The photoluminescence spectra of the SiNWs had a red emission band whose band location and shape were found to be dependent on catalyst thickness. The Raman spectra of the prepared nanowires showed that the first order transverse band shifted toward lower frequencies compared with the c-Si band location. The first order transverse band approached the c-Si band location as the wire diameter increased due to the increasing catalyst film thickness.

Keywords: Silicon nanowires, Au catalyst, optical properties, growth characteristics.

1. Introduction

In the last decade, silicon nanostructures have attracted deep interest because of their potential to be integrated as an active material for electronic and photovoltaic nanodevices [1-4] The silicon nanowire (SiNW) is one of the most attractive one-dimensional (1D) nanostructure semiconductors because of its unique electrical and optical properties which are often remarkably different from other semiconductors in the bulk phase [5]. The SiNW nanostructure was recently used to fabricate various devices such as field effect transistors, chemical sensors, and solar cells [6-8]. Compared with bulk Si, the nanowire (NW) structure exhibits an expanded direct band gap, high surface-to-volume ratio, quantum confinement effects, and slow electron–hole recombination [9, 10]. Moreover, one of the significant properties of this type of nanostructure is its efficiency as an electrical carrier. These nanostructures have high electrical mobility and high-aspect ratio morphology, which can provide direct and efficient pathways from the light-absorbing material to the conductive substrate by avoiding a series of particle-to-particle hopping transports that occur in nanoparticles [11]. Wagner and Ellis [12] first reported on a technique used to grow SiNWs based on the vapour-liquid-solid (VLS) mechanism, in which a metal catalyst plays an important role. Thus, various types of metal catalyst have been used to synthesize SiNWs. The catalysts can be classified into three groups corresponding to the metal-Si phase diagram according to the study of Schmidt et al. [13]. The phase diagram for group A, comprised of Au and Al, is dominated by a eutectic point at a Si concentration greater than 10%, and no metal-silicide phase is present [14, 15]. Group B includes catalysts such as tin (Sn) and indium (In) metals. The phase diagram for this group is dominated by a eutectic point at a low Si concentration (<1%) with the absence of silicide phases [16, 17]. The phase diagram for group C includes catalysts such as titanium (Ti) and copper (Cu) and is characterized by the

presence of one or more silicide phases with eutectic points found at temperatures above 800 °C [18, 19]. Using Au as a catalyst to synthesize SiNWs is markedly advantageous because of the low temperature eutectic point of the Au-Si phase, high Si solubility, high chemical stability of Au, and resistance to oxidation in the air [20]. Chemical vapour deposition (CVD) the most common is method used to prepare SiNWs [21]. Plasma-enhanced CVD (PECVD) is a variant of CVD and is also used to grow semiconductor NWs [22]. The assistance of plasma has numerous advantages such as reduced growth temperature, reduced oxidation on the catalyst surface, and increased growth rate of SiNWs [23]. In this report, pulsed PECVD (PPECVD) was used to grow SiNWs on ITO-glass substrates using Au thin films with varying thicknesses as the catalyst. The crystalline structure, surface morphology, and the optical properties of synthesized SiNWs were investigated.

2. Experimental Details

ITO-coated glass was used as the substrate to grow the SiNWs. The substrates were cleaned using an ultrasonic bath using decon 90, ultra-pure water, and propanol. Finally, the substrates were dried using a high-purity nitrogen flow. Then, the prepared substrates were loaded into the chamber of the thermal evaporation equipment (Bell Jar) to deposit Au thin film catalyst layer. Varying thicknesses of Au thin films (10 nm to 100 nm) were deposited on the substrates, and the thickness was controlled by a quartz crystal microbalance. To grow the SiNWs, the Au-covered ITO substrates were loaded into a PPECVD system chamber and heated to 350 °C under 3 Torr of argon pressure for 35 min. Silane (SiH_4) gas flowed into the chamber as the Si source, and the temperature was increased to approximately 400 °C. A square wave generated by a pulse generator (SRS model DG 535) was used to modulate the 13.56 MHz signal and 1 kHz modulation frequency was used to generate the plasma with approximately 30 W

power for 45 min. After the SiNW growth process was completed, the chamber was purged with argon and cooled to room temperature. The surface morphology of the grown SiNWs was revealed by field emission scanning electron microscopy (FESEM; Model FEI Nova NanoSEM 450) and transmission electron microscopy (TEM; Philips CM 100 TEM). The crystalline structure of the prepared SiNWs was investigated through X-ray diffraction (XRD) using a PANalytical X'Pert PRO MRD PW3040 instrument with CuKα radiation. The photoluminescence (PL) and Raman spectra were recorded using Horiba Jobin Yvon HR 800 UV equipment with excitation laser wavelengths of 325 and 528 nm, respectively.

3. Results and discussion

3.1 Surface Morphology

Figure 1 illustrates the FESEM images of SiNWs prepared using various thicknesses of Au thin films ranging from 10 nm to 100 nm. Homogeneous and long SiNWs were formed when 10 and 20 nm thick Au films were used (Figures 1A and 1B), similar to the SiNWs grown using 40 and 60 nm thick Au with increasing wire diameter (Figures 1C and 1D). By contrast, SiNWs catalyzed with 80 and 100 nm thick Au films demonstrated some kinking or worm-like structures especially those with 100 nm thickness (Figures 1E and 1F). Figure 2 shows the diameter distribution of the synthesized SiNWs. The diameter of SiNWs catalyzed using 10 and 20 nm thick Au ranged from 40 nm to 100 nm and 80 nm to 140 nm, respectively (Figures 2A and 2B). The increase in catalyst film thickness clearly led to an increase in the diameter of the SiNWs. The SiNWs catalyzed using 100 nm thick Au exhibited diameters ranging from 160 nm to 220 nm (Figure 2F). Cui et al. [24] synthesized SiNWs via CVD at approximately 440 °C using different Au thicknesses. They observed that an increase in the catalyst thickness from 5 nm to 30 nm resulted in an increase in the modal SiNW diameter from 6 nm to 31 nm. Moreover,

Hofmann et al. [25] used PECVD to grow SiNWs on Si wafers at 400 °C using different thicknesses of Au. They found that the modal wire diameter increased from 29 nm to 300 nm when the Au thickness was increased from 0.5 nm to 5 nm. Furthermore, Qin et al. [26] demonstrated that the diameter of SiNWs prepared via inductively coupled PCVD on Si wafers at 380 °C using 16 nm thick Au ranged from 90 nm to 130 nm and increased to 130 nm to 175 nm with a 40 nm thick Au catalyst, in agreement with our results. Al-Taay et al. [27] found that the diameter of SiNWs grown by PPECVD using a Sn catalyst also increased as the catalyst thin film thickness increased.

Figure 3 shows the relationship between the Au thickness and the modal diameter of the SiNWs. The wire diameter clearly increased when the thickness of the catalyst thin film increased. Moreover, the density of the SiNWs decreased as the Au thin film thickness increased. Thus, the wire density of SiNWs decreased from 18 NW/μm^2 to approximately 6 NW/μm^2 when 10 and 100 nm Au thicknesses were used, respectively (Figure 3). Cross-sectional FESEM images of SiNWs synthesized using 20, 60, and 100 nm thick Au catalysts are shown in Figure 4. The SiNWs were randomly oriented relative to the substrate, and the mean wire length decreased from 12 μm to approximately 10 μm as the thickness of the catalyst film increased from 20 nm to 100 nm. In addition, the images demonstrated that the grown SiNWs were tapered, and Au nanoparticles remained at the tip of the wires, indicating that the SiNWs were grown by the VLS mechanism. Figure 5 depicts the TEM images of SiNWs synthesized using 20, 60, and 100 nm thick Au catalysts. The TEM images confirmed the increase in wire diameter with an increase in the thickness of the catalyst thin film. Moreover, a tapered SiNW with a Au catalyst particle at the tip of the wire is shown. A worm-like structure was also observed in SiNWs catalyzed by 100 nm thick Au films. The eutectic temperature of the catalyst-Si system can determine the required

temperature to synthesize a SiNW via the VLS mechanism. Most metal catalysts exhibit high eutectic temperatures with Si, whereas the Au-Si system has a relatively low eutectic point of approximately 363 °C at 19% Si concentration, which is a remarkable reduction in the melting temperature compared with the melting point of Au at 1064.5 °C [13].

3.2 Crystalline Structure

The XRD patterns of the SiNWs grown using various thicknesses of Au thin film catalysts are shown in Figure 6. The diffraction peaks of the prepared SiNWs correspond to the (111), (220), and (311) lattice planes of the cubic phase of Si. The diffraction peaks became sharper as the wire diameter increased because of the increasing catalyst thickness, indicating that the crystallinity of the grown SiNWs was enhanced. The lattice constant (a) of the cubic structure is given by the relationship[28]:

$$\frac{1}{d_{hkl}^2} = \frac{h^2 + k^2 + l^2}{a^2}, \qquad 1$$

where d_{hkl} is the interplanar spacing of the atomic planes, and h, k, and l are Miller indices. The lattice constant values are listed in Table 1. Moreover, the diffraction peaks of Au related to the (111) and (200) lattice planes were also detected as shown in Fig. 6, confirming the deposition of Au particles on the top of the SiNWs. Hamodine et al. and Pham et al. [29, 30] obtained crystalline SiNWs using Au as the catalyst and synthesized by PECVD and thermal evaporation methods, respectively. The diffraction peaks of the Au catalysts appeared in the XRD patterns because the metal particles were located on top of the SiNWs. Comparing with the SiNWs prepared using Sn and Al catalysts with the same deposition conditions [9, 27] , the Au catalyst

produced the highest crystallinity SiNWs that makes it the most suitable for solar cell applications.

3.3 Photoluminescence Spectra

The photoluminescence (PL) spectra of nanocrystalline materials is one of the most effective tools for diagnosing the structure quality, surface states, and impurity levels inside the optical band gap [31]. Figure 7 shows the PL spectra of the SiNWs catalyzed using various Au thicknesses. A red emission band can be observed in the PL spectra for all the grown SiNWs. The SiNWs catalyzed by 10 nm thick Au exhibited a broad emission band that peaked at 720 nm. The PL spectrum of the SiNWs prepared using 20 nm Au catalyst showed two emission bands centered at 788 and 909 nm, whereas the grown wires using 40 nm thick Au produced bands at 752 and 890 nm. The emission bands for SiNWs catalyzed by Au layers are listed in Table 1. According to the theoretical prediction of Sanders and Chang [32], quantum confinement can be expected for nanostructure dimensions less than the free excitonic Bohr radius (5 nm) of c-Si. The diameter of the grown SiNWs is relatively larger than the Bohr radius. Thus, the quantum confinement effect is not evident. The red band was emitted because of the interface between the amorphous sheath layer and the crystalline core of the wire [33]. In the PL spectrum measured at room temperature for SiNWs synthesized by the oxide-assisted method, a main green emission band at 2.05 eV (604 nm) and a smaller red emission band at 1.7 eV (729 nm) were observed [34]. Bhattacharya et al. [35] obtained red PL emissions centered at 826 and 886 nm for different SiNW diameters, synthesized by pulsed laser vaporization using Au as catalyst. In addition, Pham et al. [30] recorded PL spectra at room temperature for SiNWs prepared by thermal evaporation using Au as the catalyst. They only obtained a broad emission band at 650 nm, and

two other bands that peaked at 455 and 510 nm were observed when measured at low temperatures.

3.4 Raman spectra

Raman spectroscopy is a powerful tool for investigating the doping concentration, lattice defect identification, and crystal orientation of materials [36]. Raman spectra of SiNWs grown using various thicknesses of Au catalyst are presented in Figure 8. The SiNWs grown using 10, 20, 40, 60, and 80 nm layers of Au produced Raman peaks located at 497, 503, 503, 505, and 507 cm^{-1}, respectively. The Raman peak was identified as the first order transverse optical phonon mode (1TO). The 1TO peak location depends on the degree of crystallinity of Si. For c-Si the 1TO peak appear at 520 cm^{-1} and for a-Si at 480 cm^{-1} [37, 38]. The Raman peak of SiNWs catalyzed by 100 nm thick Au appeared at 513.5 cm^{-1} which is shifted by approximately 6.5 cm^{-1} compared with the c-Si 1TO peak location. The wire diameter increased because of the increase in catalyst thickness, which led to an increase in the crystallinity of SiNWs that could have caused the shifting of the 1TO peak toward higher frequencies. The two broadening bands that peaked at 290 and 920 cm^{-1} are ascribed to the second order transverse acoustic phonon mode (2TA) and the second order optical phonon mode (2TO), respectively, and were observed for all prepared SiNWs [39]. Wang et al. [40] found that the Raman peak location is dependent on the diameter of the wires synthesized by laser ablation, and the Raman peak appeared at 509.8 cm^{-1} for 10 nm wide NW and shifted to 517.7 cm^{-1} when the diameter of the wires increased to 21 nm. Meshram et al. [41] obtained a Raman peak at 515 cm^{-1} for NWs with diameters ranging from 50 nm to 300 nm for SiNWs grown at 400 °C by hot wire CVD. Moreover, a sharp Raman peak at 500 cm^{-1} for SiNWs synthesized by PECVD at 400 °C with diameters ranging from 40 nm to

400 nm was also observed[14]. The crystallite size D_r, can be estimated, depending on the value of the shift in TO phonon mode [42]:

$$D_r = 2\pi\sqrt{\frac{B}{\Delta\omega}}, \qquad 2$$

where B is 2.24 cm^{-1} nm^2 for Si and $\Delta\omega$ is the shift of the TO peak from the c-Si peak location. The crystallite size increased from 1.9 nm for the wires grown using a 10 nm thick Au catalyst to 3.22 nm for the wires catalyzed by a 100 nm thick Au catalyst (Table 1). The increase in crystallite size when the Au catalyst thickness increased implies enhanced crystallinity of the SiNWs grown with an increased catalyst thickness, as illustrated also in the XRD patterns. Chong et al. [43] prepared SiNWs using 50 nm to 250 nm In droplet size with a home-built hot-wire-assisted PEVCD system. They concluded that the SiNWs grown using 40W rf power had high crystallinity with a crystallite size of 4.2 nm compared with those was prepared using 80W rf power with crystallite size of 2.9 nm. Moreover, they noted that the TO band of the SiNWs grown using low rf power was located at 517 cm^{-1}, whereas the band peaked at 512 cm^{-1} for the wires synthesized using high rf power.

4. Conclusions

Varying thicknesses of the Au catalyst ranging from 10 nm to 100 nm have been used to synthesize SiNWs via the PPECVD method at 400 °C. FESEM and TEM images confirmed that the wire diameter increased as the thickness of the catalyst film increased, and the wire length

decreased from 12 μm to approximately 10 μm. The presence of Au nanoparticles at the tips of the wires indicates that the SiNWs were grown via the VLS mechanism. XRD patterns showed that the synthesized SiNWs consisted primarily of crystalline Si with (111), (220), and (311) growth planes. The SiNWs grown by Au catalyst had high crystallinity which makes them suitable for fabricating a solar cell. The PL spectra of the SiNWs prepared with various Au thicknesses showed red emission bands. Raman spectroscopy confirmed the increase in crystallinity of the SiNWs as the Raman peaks shifted from 497 cm^{-1} to 513.5 cm^{-1} as the catalyst thickness increased.

References

[1] A.B. Jaballah, B. Moumni, B. Bessais, Solar Energy 85 (2012) 1955-1961.

[2] A. Ramizy, Z. Hassan, K. Omar, Y. Al-Douri, M.A. Mahdi, Applied Surface Science, 257 (2011) 6112-6117.

[3] B.R. Mohamed, H. Anouar, B. Brahim, Solar Energy, 86 (2012) 1411-1415.

[4] Ian Y.Y. Bu, T.J. Hsueh, Solar Energy, 86 (2012) 1454-1458.

[5] J. David, Device Applications of Silicon Nanocrystals and Nanostructures, Ottawa,Ontario, Canada, 2009.

[6] S. Sato, H. Kamimura, H. Arai, K.Kakushima, P. Ahmet, K. Ohmori, K. Yamada, H. Lwai, Solid State Electronic, 54 (2010) 925-928.

[7] A. Agarwal, K. Buddharaju, I. K. Lao, N. Singh, N. Balasubramanian, D. L. Kwong, Sensor and Actuators A:Physical, 145-146 (2008) 207-213.

[8] T.J. Kempa, B. Tian, D.R. Kim, J. Hu, X. Zheng, C.M. Lieber, Nano Letters, 8 (2008) 3456-3460.

[9] H.F. Al-Taay, M.A. Mahdi, D. Parlevliet, Z. Hassan, P. Jennings, A. Agarwal, Physica E, 48 (2013) 21-28.

[10] D.D.L. Ma, C.S. Au, F.C. Tong, S.Y. Lee, S.T., Science, 200 (2003) 1874-1877.

[11] M.A. Mahdi, J.J. Hassan, S.S. Ng, Z. Hassan, Journal of Crystal Growth, 359 (2012) 43-48.

[12] R.S. Wagner, W.C. Ellis, K.A. Jackson, S.M. Arnold, Journal of Applied Phyics, 35 (1964) 2993-3000.

[13] V. Schmidt, J.V. Wittemann, S. Senz, U. Gosole, Advanced Materials, 21 (2009) 2681-2702.

[14] S.K. Chong, B.T. Goh, Z. Aspanut, M.R. Mahamed, C.F. Dee, S.A. Rahman, Thin Solid Films, 519 (2011) 4933-4939.

[15] S.Y. Choi, W.Y. Fung, W. Lu, Applied Physics Letters, , 98 (2011) 033108-033101.

[16] L. Yu, P.J. Alet, G. Picardi, I. Maurin, P.R.I. Cabarrocas, Nanotechnology, , 19 (2008) 485605 (485605pp).

[17] M. Jeon, K. Kamisako, Materials Letters, 62 (2008) 3903-3905.

[18] S. Sharma, T.I. Kamins, R.S. Williams, Journal of Crystal Growth, 267 (2004) 613-618.

[19] Y. Yao, S. Fan, Materials Letters, 61 (2007) 177-181.

[20] V. Schmidt, J.V. Wittemann, U. Gosele, Chemical Review, 110 (2010) 361-388.

[21] D. Kohen, C. Cayron, E.D. Vito, V. Tileli, P. Faucheraud, C. Morin, A. Brioude, S. Perraud, Journal of Crystal Growth, 341 (2012) 12-18.

[22] J.S. Jie, W.J. Zhang, Y. Jiang, X.M. Meng, J.A. Zapien, M.W. Shao, S.T. Lee, Nanotechnology, 17 (2006) 2913-2917.

[23] S. Hofmann, C. Ducati, J. Robertson, B. Kleinsorge, Applied Physics Letters, 83 (2003) 135-137.

[24] Y. Cui, L.J. Lauhon, M.S. Gudiksen, J. Wang, C.M. Lieber, Applied Physics Letters, 78 (2001) 2214-2216.

[25] S. Hofmann, C. Ducati, R.J. Neill, S. Piscanec, A.C. Ferrari, J. Geng, R.E.D. Borkowski, J. Robertson, Journal of Applied Physics, 94 (2003) 6005-6012.

[26] Y. Qin, F. Li, D. Liu, H. Yan, J. Wang, D. He, Materials Letters, 65 (2011) 1117-1119.

[27] H.F. Al-Taay, M.A. Mahdi, D. Parlevliet, P. Jennings, Materials Science in Semiconductor Processing 16 (2013) 15-22.

[28] B.D. Cullity, Elements of X-Ray Diffraction, Addison-Wesley, Reading, MA, USA, 1972.

[29] H. Hamidinezhad, Y. Wahab, Z. Othaman, A.K. Ismail, Applied Surface Science, 257 (2011) 9188-9192.

[30] V.T. Pham, V.N. Le, A.T. Chu, T.T. Pham, N.K. Tran, H.D. Pham, T.H. Pham, Advances in Natural Sciences: Nanotechnol and Nanasecience

2(2011) 015016-015021.

[31] M.A. Mahdi, J.J. Hassan, S.S. Ng, Z. Hassan, N.M. Ahmed, Physica E, 44 (2012) 1716-1721.

[32] G.D. Sanders, Y.C. Chang, Physical Review B, 45 (1992) 9202-9213.

[33] F. Shi, J. Lin, Y. Huang, J. Zhang, C. Tang, Materials Chemistry and Physics, 118 (2009) 125-128.

[34] A. Coll, S. Hofmann, A.C. Ferrari, C. Ducati, R.E.D. Borkowski, J. Robertson, Applied Physics A 85 (2006) 247-253.

[35] S. Bhattacharya, D. Banerjee, K. W. Adu, S. Samui, S. Bhattacharyya, Applied Physics Letters, 85 (2004) 2008-2010.

[36] M.A. Mahdi, Z. Hassan, S.S. Ng, J.J. Hassan, S.K. Mohd Bakhori, Thin Solid Films, 520 (2012) 3477-3484.

[37] Z.Q. Liu, S.S. Xie, W.Y. Zhou, L.F. Sun, Y.B. Li, D.S. Tang, X.P. Zou, C.Y. Wang, G. Wang, Journal of Crystal Growth, 224 (2001) 230-234.

[38] C.T. Li, F. Hsieh, L. Wang, Solar Energy, 88 (2013) 104-109.

[39] B.B. Li, D.P. Yu, S.L. Zhang, Physical Review B, 59 (1999) 1645-1648.

[40] R.P. Wang, G.W. Zhou, Y.L. Liu, S.H. Pan, H.Z. Zhang, D.P. Yu, Z. Zhang, Physical Review B, 61 (2000) 16827-16832.

[41] N. P. Meshram, A. Kumbhar, R.O. Dusane, Thin Soild Films, 519 (2011) 4609-4612.

[42] S.K. Chong, B.T. Goh, Z. Aspanut, M.R. Muhamad, C.F. Dee, S.A. Rahman, Applied Surface Science, 257 (2011) 3320-3324.

[43] S.K. Chong, B.T. Goh, Y.Y. Wong, H.Q. Nguyen, H. Do, Z. Aspanut, M.R. Muhamad, C.F. Dee, S.A. Rahman, I. Ahmad, A. Agarwal, Journal of Luminescence, 132 (2012) 1345-1352.

Figure captions

Figure 1: FESEM images for SiNWs prepared using Au catalyst layer thicknesses of (A) 10 nm, (B) 20 nm, (C) 40 nm, (D) 60 nm, (E) 80 nm and (F) 100 nm.

Figure 2: Diameter distribution of SiNWs grown using Au catalyst layer thicknesses of (A) 10 nm, (B) 20 nm, (C) 40 nm, (D) 60 nm, (E) 80 nm and (F) 100 nm.

Figure 3: The Au catalyst thin film thickness vs. wire diameter and density.

Figure 4: Cross-sectional images for SiNWs synthesized using Au catalyst layer thicknesses of (A) 20 nm, (B) 60 nm and (C) 100 nm.

Figure 5: TEM images of SiNWs prepared by Au catalyst layer thicknesses of (A) 20 nm, (B) 60 nm and (C) 100 nm.

Figure 6: XRD patterns of SiNWs prepared using Au catalyst layers with thicknesses 10-100 nm.

Figure 7: Room temperature PL spectra of the SiNWs grown using Au catalyst layer thicknesses of (A) 10 nm, (B) 20 nm, (C) 40 nm, (D) 60 nm, (E) 80 nm and (F) 100 nm.

Figure 8: Raman spectra of SiNWs prepared using an Au catalyst layers with thicknesses of 10 nm, 20 nm, 40 nm, 60 nm, 80 nm and 100 nm.

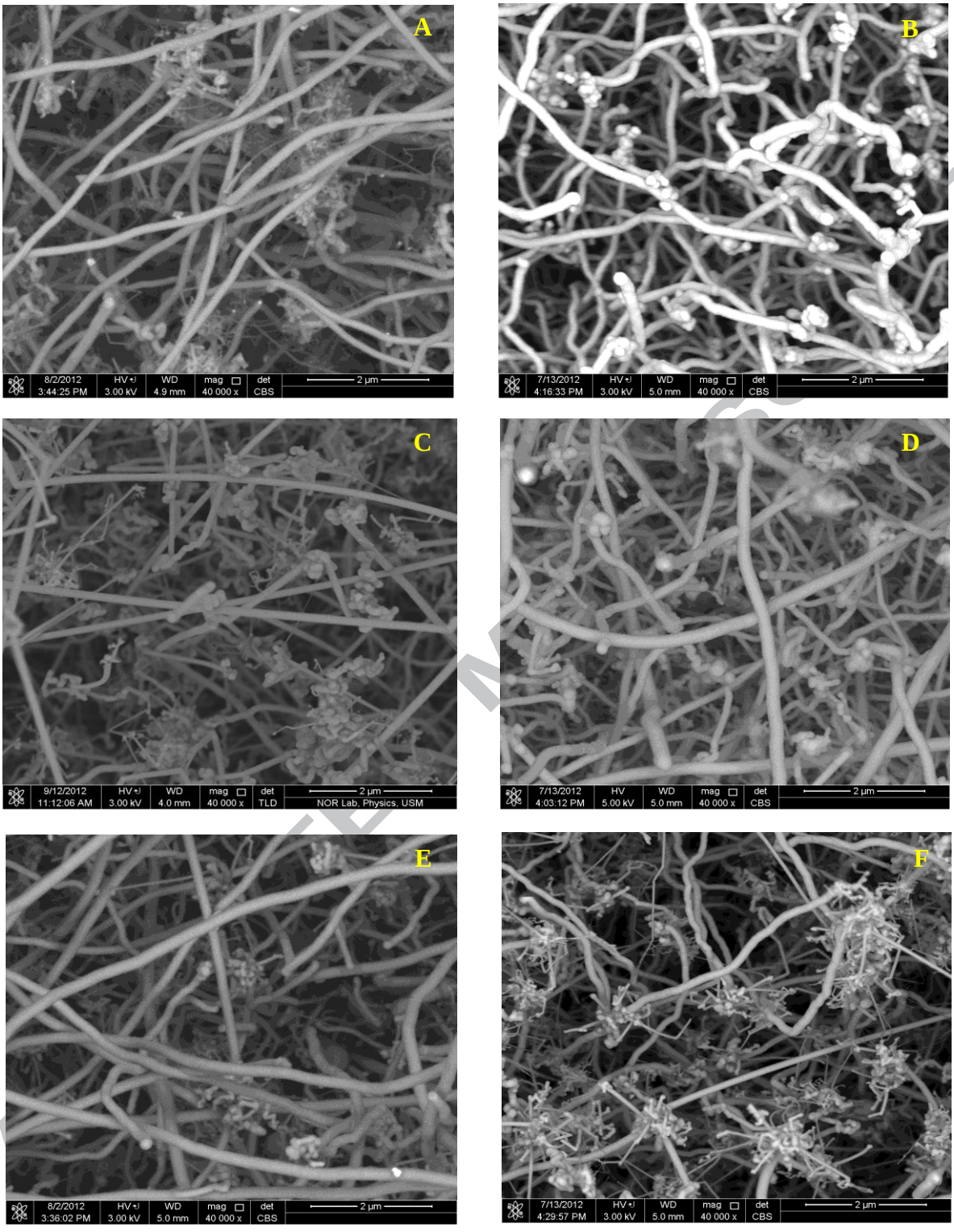

Fig. 1

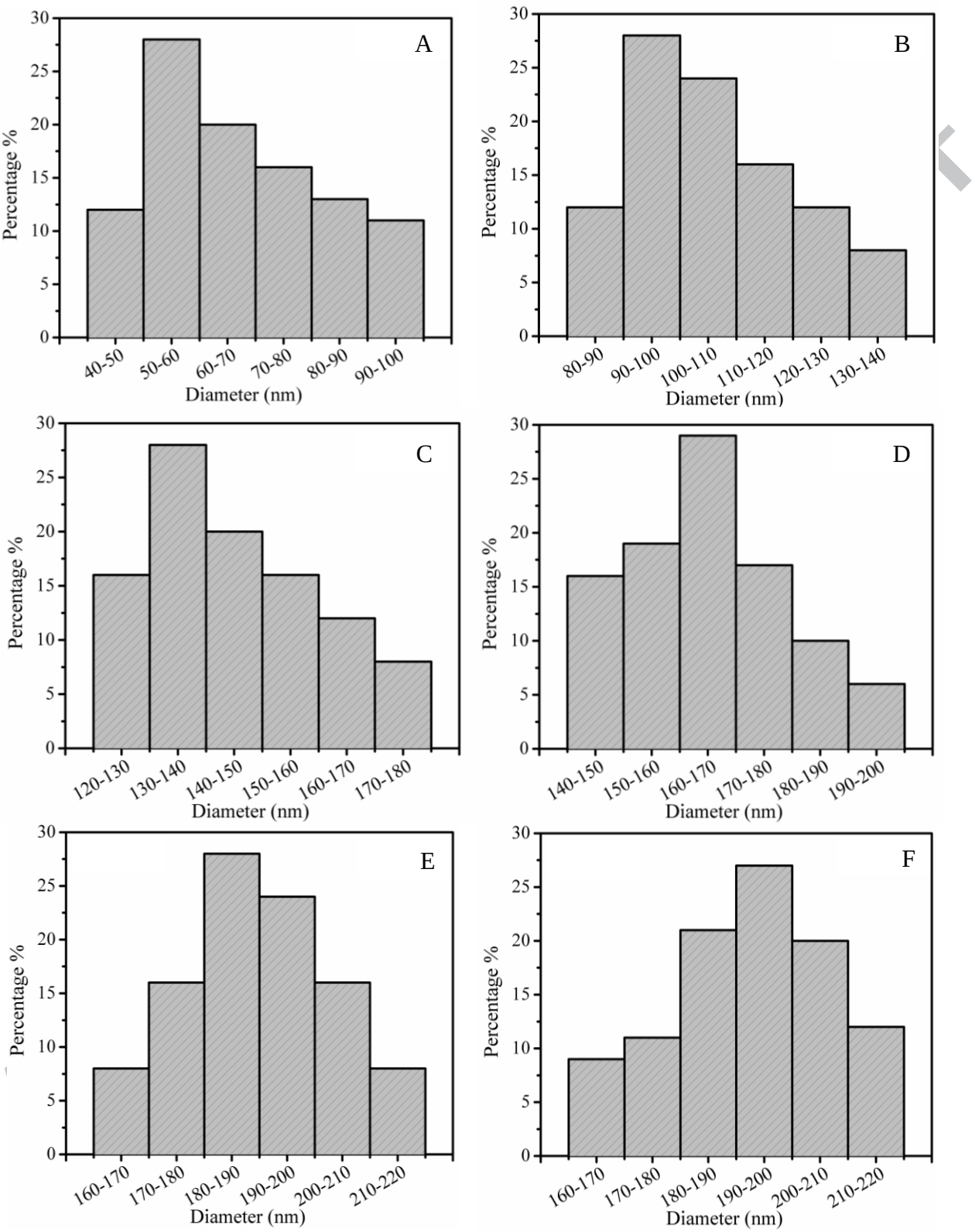

Fig. 2:

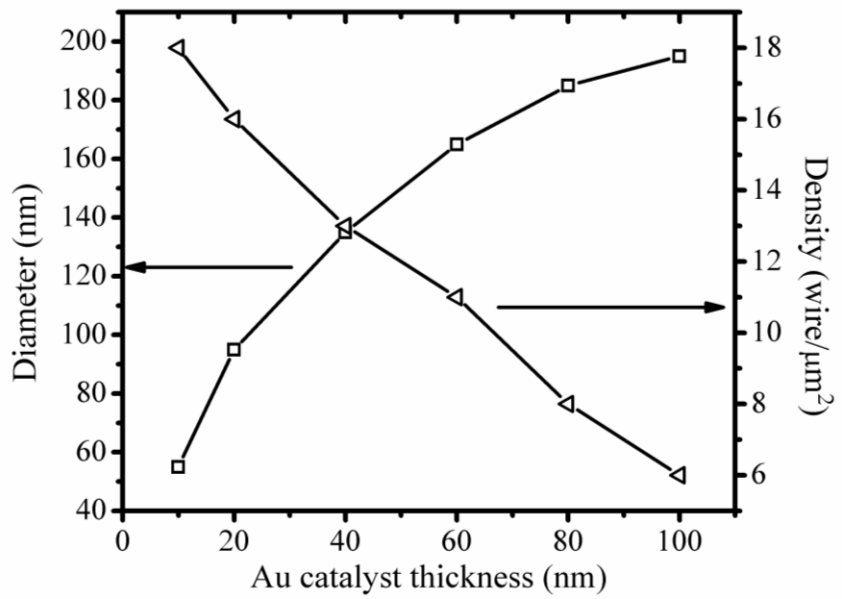

Fig. 3:

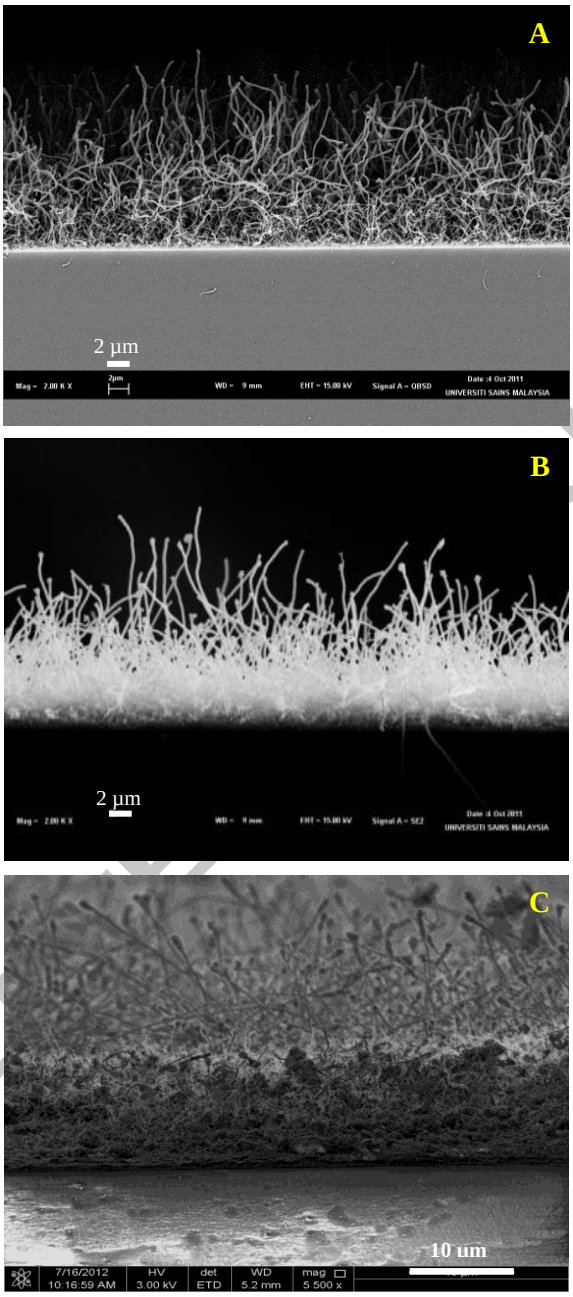

Fig. 4:

Fig. 5:

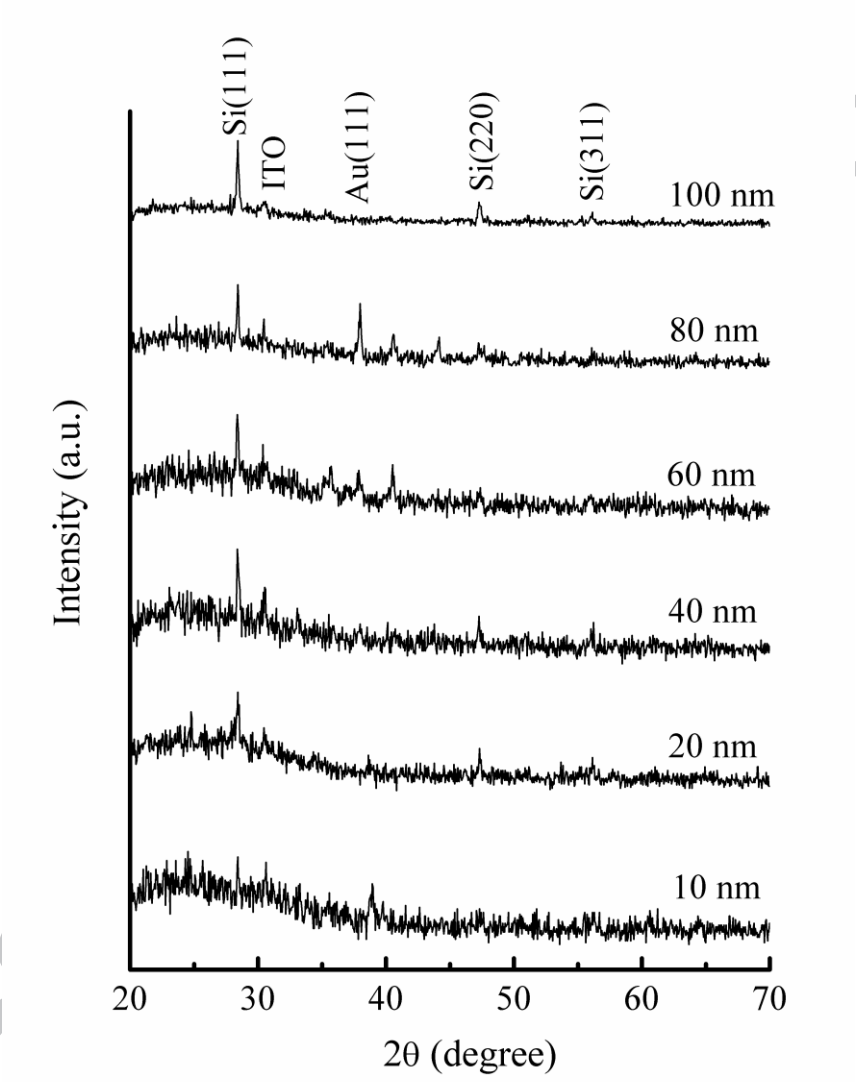

Fig. 6:

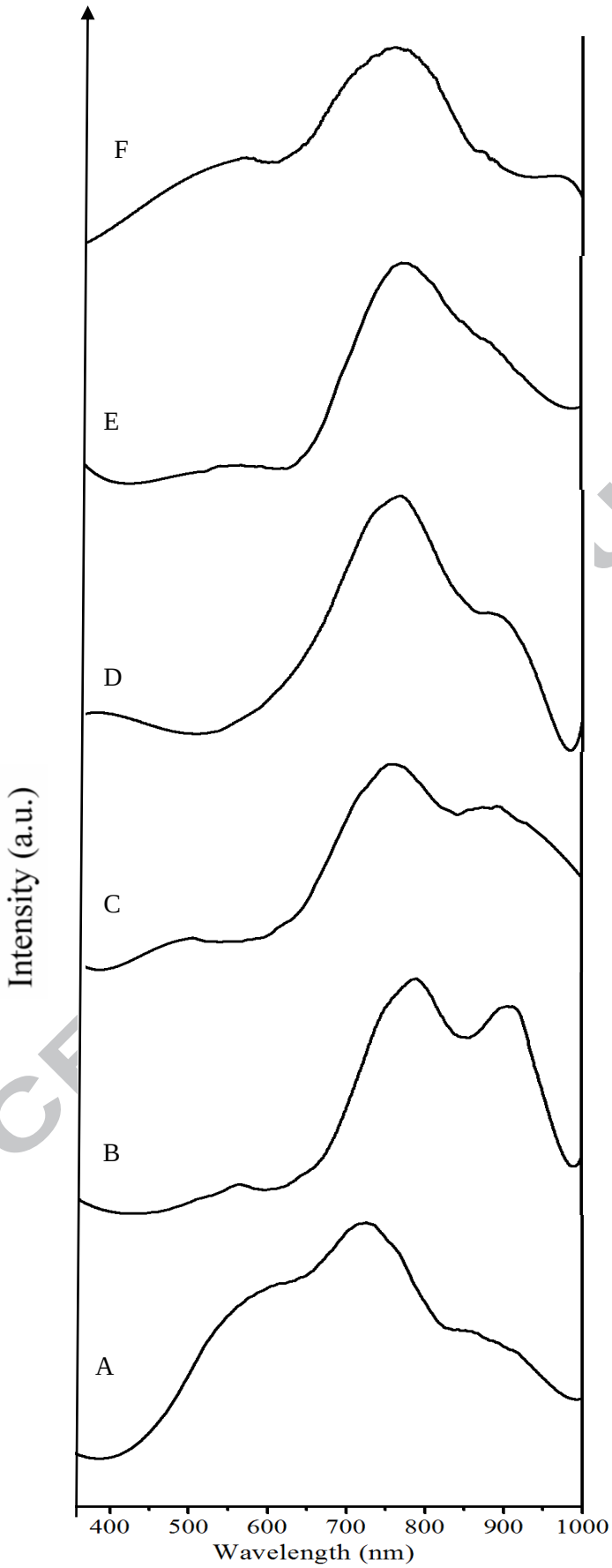

Fig. 7:

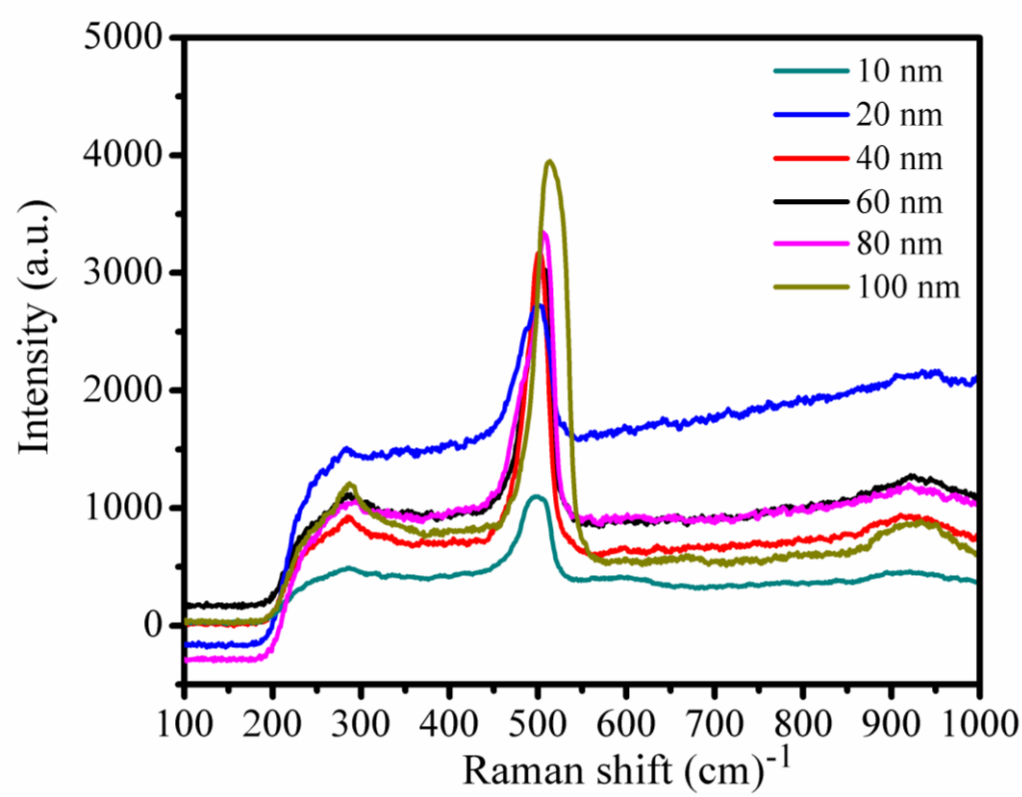

Fig. 8:

Table caption

Table 1: Peak locations of the Raman and PL bands for SiNWs grown with an Au thin film catalyst of different thicknesses

Table 1:

Catalyst thickness (nm)	Lattice constant (□)	FWHM of (111) XRD peak(degree)	PL bands (nm)	Raman band cm^{-1}	D_r (nm)
10	5.430	0.221	720	496.5	1.9
20	3.438	0.210	788, 909	503	2.21
40	5.435	0.198	752, 890	503	2.21
60	5.438	0.197	761, 881	505	2.35
80	5.445	0.190	762	507	2.51
100	5.438	0.182	750	513.5	3.22

.

Highlights

> Silicon nanowires (SiNWs) were grown by PPECVD>A gold (Au) metal was used as a catalyst> The wire diameter increased as the catalyst film thickness increased > Increasing the catalyst thickness led to enhanced the crystallinityof the wires>The Raman spectra of the prepared nanowires was studied>